DEGREE PROJECT IN CHEMICAL SCIENCE AND ENGINEERING, SECOND CYCLE, 30 CREDITS

STOCKHOLM, SWEDEN 2020

Towards a virtual climate chamber

A physical experimental study

JAVIER ARROYO MOLINA

KTH ROYAL INSTITUTE OF TECHNOLOGY
SCHOOL OF ENGINEERING SCIENCES IN CHEMISTRY, BIOTECHNOLOGY AND HEALTH

TRITA CBH-GRU-2020:222

Master in Chemical Engineering for Energy and Environment

June 30, 2020

Work proposed by Ericsson AB, Thermal Design Department

Developed in Ericsson AB, Kista, Stockholm

Supervisors: Stevin Van Wyk and Mireia Altimira, Ericsson AB

Examiner: Matthäus Bäbler, KTH Royal Institute of Technology

School of Engineering Sciences in Chemistry, Biotechnology and Health

ERICSSON

Abstract

Thermal cooling is a hot topic in the electronics world. So that electronic equipment can become more powerful and compact, the heat generated during operation must be dissipated effectively. This is a key aspect in the Thermal Design department at Ericsson AB, a research and development sector which is in need of constant upgrades of their performance analysis techniques, so that their products are competitive in the electronics market.

This project focuses on experimentally characterizing one of the tools used in Ericsson AB to test product performance, the climatic chamber. By conducting experiments inside the climate chamber and post processing the data obtained, the airflow inside it can be understood and compared to outdoor experimental data. One of the main sections of this work is to prove the hypothesis: 'The energy potential of the wind outdoors is greater than indoors', which is shown to be true when comparing values for the integral length scales of the flow, at the same mean wind speed.

The second main part of this project is to obtain valuable experimental input that will serve to construct a virtual model of the climate chamber. With the conclusions drawn from the experiments, which involve heat transfer, boundary conditions for the numerical model can be established. The final section of this report includes a comparison between the results obtained from the experimental analysis and the numerical model. These results match for certain conditions of the wind flow, for a 50% fan power configuration and in positions close to the front door of the climate chamber, but more work has to be done so that the results obtained from both experiences are more matching.

Towards a virtual climate chamber is the first step in an iterative process involving experimental and numerical work. As of now, the basis has been laid in obtaining a valid model of the airflow in the climate chamber. Future recommendations towards this goal are explained in the final section of this project, which will involve more experimental work on how the air dissipates heat from electronic equipment, regardless of their shape and orientation.

Sammanfattning

Det talas mycket om Termisk kylning inom elektronikvärlden. För att elektronisk utrustning ska kunna bli mer kraftfull och kompakt, måste värmen som genereras under arbetet spridas effektivt. Detta är en av de centrala aspekten inom avdelningen för Termisk Design på Ericsson AB, en forsknings- och utvecklingssektor som är i behov av ständiga uppgraderingar av prestanda-analys tekniker, för att bibehålla produkternas konkurrenskraft på elektronikmarknaden.

Det här projektet fokuserar på att experimentellt karakterisera ett av verktygen som används i Ericsson AB för att testa produktprestanda - klimatkammaren. Genom att utföra experiment inuti klimatkammaren och efterbehandla de erhållna data, kan man få en förståelse för luftflödet inuti kammaren och jämföra resultat med experimentella data från utomhus. Ett av delmomenten i detta arbete bevisar hypotesen: 'Vindens energipotential är större än inomhus', vilket visar sig vara sant när man jämför värden för flödets integrala längdskalor, med samma medelvärde i vindhastighet.

Den andra etappen av detta projekt är att erhålla en värdefull experimentell vägledning som kommer att tjäna till att konstruera en virtuell modell av klimatkammaren. Med slutsatserna från experimenten, som innefattar värmeöverföring, kan gränsvillkor för den numeriska modellen fastställas. Det sista avsnittet i denna rapport innehåller en jämförelse mellan resultaten som erhållits från den experimentella analysen och den numeriska modellen. Dessa resultat matchar för vissa förhållanden i vindflödet: för en 50% fläktkraftkonfiguration och i lägen nära klimatkammarens ytterdörr. Men mer arbete måste utföras för att bekräfta hur mycket resultaten från båda erfarenheterna egentligen matchar.

Det här arbetet mot en virtuell klimatkammare är det första steget i en iterativ process som involverar experimentellt och numeriskt arbete. Från och med nu har grunden lagts för att erhålla en giltig modell av luftflödet i klimatkammaren. Framtida rekommendationer mot detta mål förklaras i det sista avsnittet av detta projekt, som kommer att involvera mer experimentellt arbete med hur luften sprider värme från elektronisk utrustning, oavsett form och orientering.

Table of Contents

Chapter 1

Introduction

The Encyclopedia Britannica, described as the world standard in knowledge since 1768 [1], describes social change as ''the alteration of mechanisms within the social structure'', an ongoing dynamic process since the emergence of humankind. However, the rate of change of social behaviour varies greatly from era to era. Throughout modern history, technological advancements have been the main motor of societal change; the faster technology develops, the more advanced the society becomes. It is exciting to feel that we are riding the wave of our own societal change, but it is breathtaking to realize the rate at which all of our lives will have to adapt. Nonetheless, all these improvements are necessary when considering the future of humankind, to fulfill our role as explorers and to keep progressing towards a brighter tomorrow.

As electronic equipment becomes more powerful and compact, larger quantities of heat are generated per unit volume. Being able to dissipate this heat effectively is what determines how competitive a specific product is, when comparing similar electronic apparatus. In the thermal design department at Ericsson AB, where this thesis is conducted, the main focus is on designing heat sinks for different Ericsson AB products. The objective is to dissipate the heat generated in electronic components as efficiently as possible in the real environment.

Thermal cooling of electronic equipment is part of the research and development (R&D) sector at Ericsson AB, where new ideas and designs must be developed to keep up with the demands of the advancement of electronic equipment. Hence, it is very important that the tools that designers use are also getting upgraded. Upgrades in the performance analysis, testing techniques and effectiveness of tools are necessary for designers to meet Ericsson AB standards in the vying electronics market.

Climate chambers are one of the main tools which Ericsson AB utilizes in order to test product performance. These walk-in climate chambers are physical tools which allow carrying out experiments to simulate natural convection conditions that prevail outdoors, in controlled laboratory environments. Setting the parameters of the climate chambers in a certain manner, allows to carry out tests that serve as validation of the correct outdoor operation of the units.

Another tool which is useful in thermal cooling design is Computational Fluid Dynamics (CFD). This**,** on the other hand, is a numerical tool. CFD has a reliable and versatile nature of application, it can be used for any scenario where modelling of the fluid behavior

is required to capture the heat transfer. Compared to conventional testing tools and procedures, it is a very efficient technique as it increases effectiveness and improves the analysis of the results in several ways. It allows to visualize the flow behavior, change design parameters quickly, iterate the results based on the analysis and therefore empower the design process greatly.

This thesis report will focus on the physical experimental study of one of the climate chamber at Ericsson AB. However, parallelly to this project, another thesis work is carried out on obtaining a numerical CFD model which reflects the behaviour of the airflow inside this climate chamber [12]. The numerical simulation study will be used as a reference in the conclusions of this text. Both thesis works are seen as one individual project in Ericsson AB, with the title 'Towards a Virtual Climate Chamber'.

1.1 Motivation

'Towards a Virtual Climate Chamber' was conceived as one plan but split into two main tasks due to its relevance in separate engineering fields. The main purpose in carrying out this project is to fill the knowledge gap accumulated using conventional testing techniques; to gain understanding on how a virtual climate chamber model can emulate a physical climate chamber or the outdoors, with reasonable resources. Conventional testing techniques refer to both physical experiments and CFD analysis, the study of how these tools combine is the central motivation of the research project.

Additionally, it is equally important for this project to serve as a first step in empowering the design process of heat sinks and other thermal cooling methodologies within the electronics design. To visualize the flow in wind like environments using commercial CFD packages and experimental data as input. At the same time, this will alleviate the usage of climate chambers for such performance analysis, as the amount of physical climate chambers is much more limited than the amount of computational resources in Ericsson AB.

1.2 Aim and Delimitations

The main goals of this thesis work are:

- Planning experiments which will be conducted inside the Ericsson AB climate chamber while keeping internal validity high and establishing control successfully in each test.
- Post processing the experimental data, to understand and derive the characteristics of the flow circulating during the testing of equipment, which involving heat transfer.
- Quantify and compare the experimental results obtained with actual outdoor data previously obtained by Ericsson AB. This will serve to demonstrate the hypothesis: The energy potential of the wind outdoors is greater than indoors.

- Describe what future steps must be conducted to build upon the developed model and understand the limitations of this tool.

This project should be considered as a necessary first step in developing the virtual climate chamber model. The main concern is to understand the extent to which this idea is realizable, attempting to obtain a fail-safe model which reflects certain experimental conditions. Any assumptions made will be explained in detail.

This project is bound to a 20 week time limit, but it is important to note that it was realized during the COVID-19 pandemic, which limited the amount of resources that could be used.

1.3 Outline

- This thesis starts with an introduction to thermal electronic design and the tools used, as well as with the motivation of the project and the goals towards its completion in Chapter 1.
- Chapter 2 describes the equipment used, the experimental strategy and the methods followed in analyzing the data, which will include a theoretical approach to the turbulent behavior of the wind.
- Chapter 3 will focus on the results obtained experimentally and on the discussion of what the values mean. This chapter includes the comparison between outdoor wind data and indoor wind data. Here is where the hypothesis regarding energy potential of the wind is demonstrated.
- Chapter 4 includes the conclusions obtained from this project, which includes a small section on how the results of this work and the numerical work developed parallelly [12] combine into a final result. Also the recommendations are discussed here, regarding the main points left to do in order for advancing 'Towards a Virtual Climate Chamber´.

Chapter 2

Tools and methods

This chapter describes the apparatus, experiments conducted and methods used to post process the data obtained experimentally. It is divided in three parts:

- The first part describes the climate chamber and the equipment utilized.

It is important to first understand how the climate chamber works, to predict how the flow inside will develop. The description of how it functions will start with an overview of the dimensions and key components, followed by a more detailed explanation on the settings and an overview on how the fans pump air in and out of the chamber is conducted. The measurement apparatus will also be described in this section.

- The second part describes the experiments carried out.

This part will display the experimental strategy and experimental procedure, how the apparatus is used and how the data is collected. Results from the tests will be compared to previous experiments carried out by the Thermal Design department at Ericsson AB, and so it is crucial that the practices applied in this work and in earlier experiments are similar.

- The third part describes the methods utilized to analyze the data and the theory behind it.

Here, the relevant turbulence theory is explained, which justifies the data post processing.

2.1 Climate chamber

On the premises of Ericsson AB, in Kista Science City, there are many walk in climate chambers installed. This thesis work will focus on only one of them; the description of the operation and the performance of tests will only be done on a specific climate chamber unit, that is accessible by the thermal design department.

Climate chambers can be described as closed-circuit environments in which test subjects are introduced and then subjected to a wide range of environmental conditions. Climate chambers are normally used in Ericsson AB to bench test products in the last stages of product design, for extreme working conditions, by changing the operating parameters (velocity of air, temperature and humidity) and therefore serve as validation for the well-functioning of the product. The interior of the climate chamber, where the elements are placed and the airflow develops, is known as test chamber.

The manufacturer of the climate chamber is Vöstch Industrietechnik (Balingen, Germany). The model of the climate chamber is VCZ 50040-S. The information shown in this chapter is extracted from the 'operating manual' [2], from the calibration protocol (carried out by LaboTest (Väsby, Sweden)) [3] and from the experience gained by physically exploring the climate chamber.

Dimensions and components

The schematic structure of the climate chamber is illustrated in figure 1, 2 and 3, where the front, right and top view are shown respectively [2].

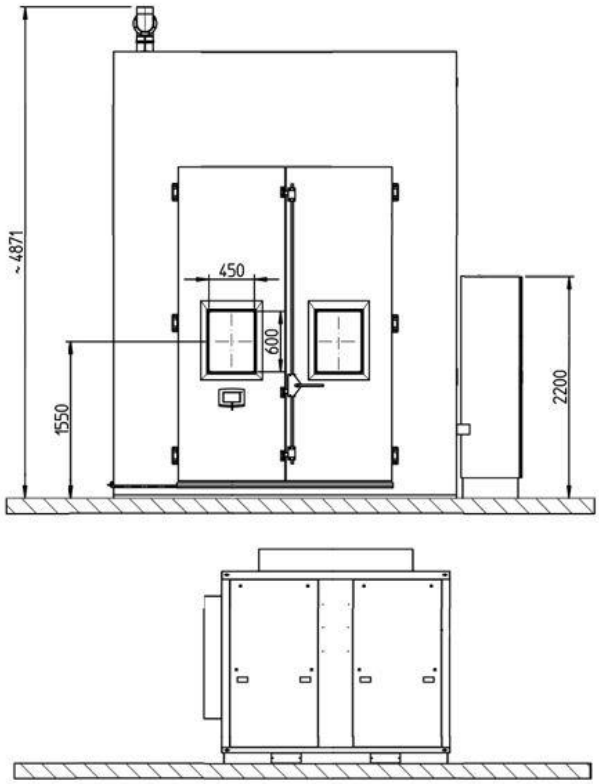

Figure 1. Climate chamber VCZ 50040-S front view. Distances are in mm. [2].

Figure 1 illustrates the front view of the climate chamber, which shows:

- Test room door and windows.
- Exhaust air opening, on the topmost left part.
- Switch cabinet, outside of the chamber, to the right.
- Machine cabinet situated underground.

The door can be opened fully, after engaging the pressure door seal.

The exhaust air opening allows for fresh air to flow into the chamber and therefore accounts for the equalization of the pressure in the test space.

The switch cabinet acts as housing for the interior electrical components that constitute the switchgear of the climate chamber.

The machine cabinet contains the cooling water connections.

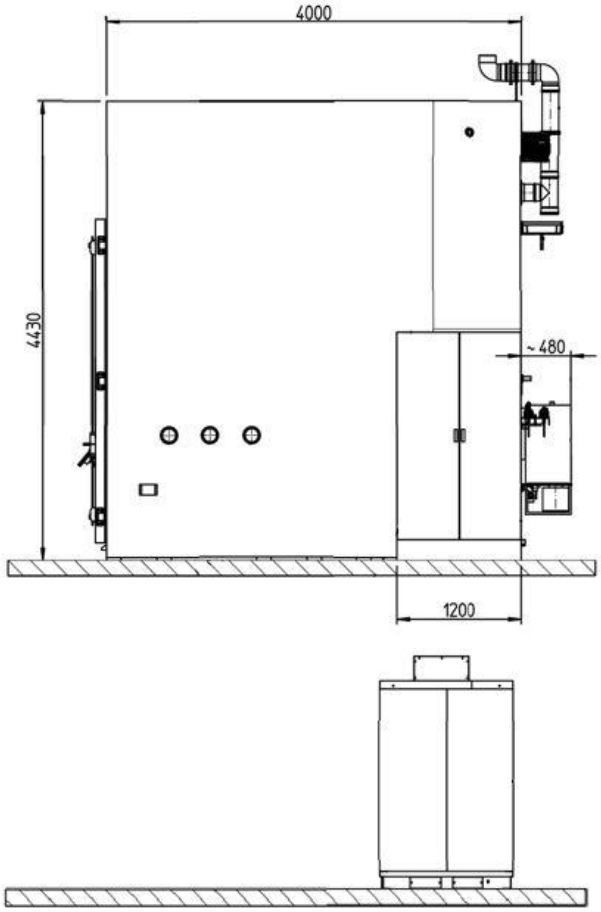

Figure 2. Climate chamber VCZ 50040-S right view. Distances are in mm. [2].

Figure 2 illustrates the right-side view of the climate chamber, which shows:

- Three grommets in the right-side wall
- Pressurized air inlet to the chamber, on the top
- Water inlet to the chamber, on the bottom
- Machine cabinet situated underground

The grommets act as access ports so that equipment can be connected from the outside without experiencing any temperature drops. They are used in this thesis work to connect the measuring equipment inside the chamber, to the power supply and recording equipment outside.

The water and air inlets are shown to the right of the figure but will not be explained any further as they are not relevant for the measurements.

The side view of the underground machine cabinet is also present.

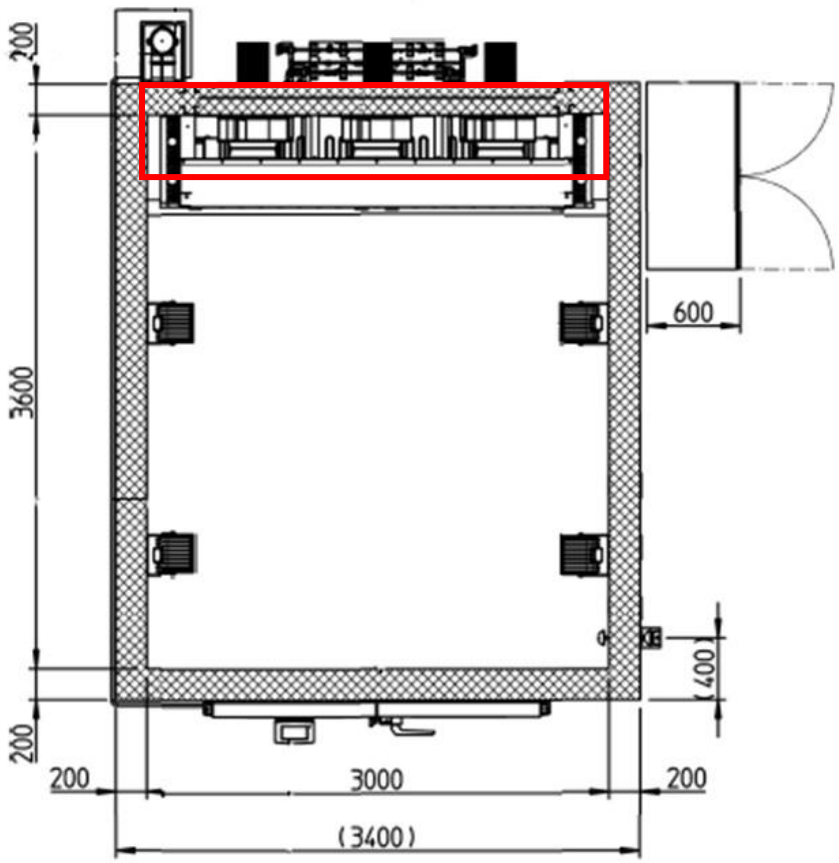

Figure 3. Climate chamber VCZ 50040-S top view. Distances are in mm. [2].

Figure 3 illustrates the top view of the climate chamber, which shows:

- Test chamber
- Fans

Figure 3 mainly shows the test space inside the chamber, along with the elements that compose it (lights, emergency door opener and fans).

The most important features for the experimental work are the test chamber and the fans. A more detailed explanation on how the fans function is done in section 2.1.3, but as an overview, the top view of the fans is shown enclosed in the red rectangle, along the back wall of the chamber. The climate chamber contains 3 fans in the topmost part of the back wall.

Technical data

It is crucial for Ericsson AB operation that the climate chamber functions precisely as the manufacturer specified in the 'operating manual'. In this manual, all data regarding its functioning is presented; general data, mechanical load data, operating data, noise measurement, data for compressed air, data for temperature tests, data for climate tests and information on cooling water.

The characterization of the climate chamber is done as follows:

- Ambient indoor conditions (25°C, 1Bar, 50%RH)

- In the volume of the test chamber (36m^3)
- Varying fan power configurations (30%, 50%, 100%)
- With the presence of a heat source (radio mock-up unit)

Through the control panel outside the chamber, the temperature and humidity inside can be monitored. The climate chamber is designed to be a fully closed airflow circulation loop, every parameter can be programmed from the control panel outside. This efficient monitoring system exerts control over every experimental variable, and therefore there is no need to set a further control room.

Before any characterization tests were performed, the company LaboTest oversaw carrying out the calibration of the temperature and humidity parameters in the climate chamber. Following the calibration protocol, temperature and humidity sensors were placed in different locations in the test chamber, to measure the difference between the conditions inside the chamber and what the control panel reads.

Temperature calibration tests were carried out at -45 °C, +30 °C and +60 °C. Humidity calibration tests were carried out at 95%rF and at 40%rF. From the calibration protocol document, and for every scenario tested, both humidity and temperature readings match with what the control panel specifies [2]. This means that there is certainty that the temperature and humidity values in the test chamber can be accurately read from the control panel outside. This will be used throughout the characterization tests to check if the conditions mentioned are constant in every experience.

Fans functioning

Air is pumped in and out of the test chamber with the use of fans. The main independent variable in the airflow characterization tests is the fan power. From one experiment to the other, the main change in the airflow corresponds to changes in the fan power settings. The airflow is the dependent variable while the fan power is the independent variable. The fan power can be set from the control panel. Information on fan performance cannot be found on the chamber's 'operating manual', the fans are manufactured by a different company and therefore technical data on their operation is not present in said manual.

The first step in the process is to physically observe how the fans function. Figures 4 and 5 show the back wall of the chamber, including the position of the fans and how the components look like after the metallic plate in the middle is unscrewed.

Figure 4. Climate chamber back wall

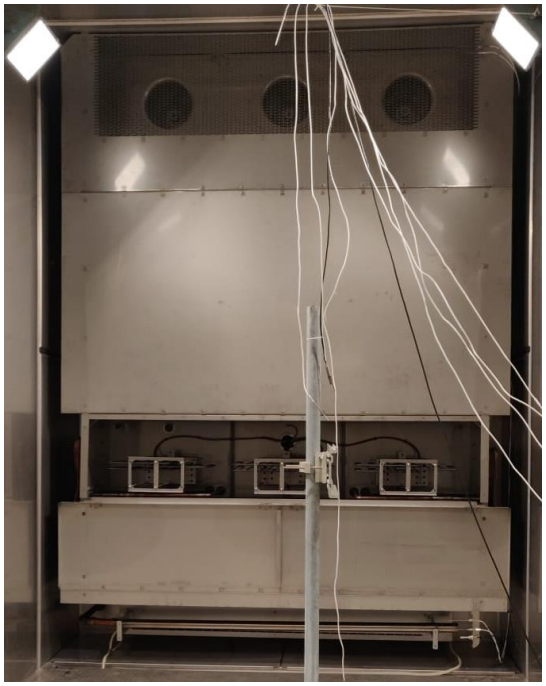

Figure 5. Back wall with middle unscrewed

The three fans are shown at the top of figures 4 and 5. Air is sucked from the top, through the opening in the fans. This same air is then pushed downwards by the fans, in a vertical manner and towards the downmost part of the back wall. Therefore the air inlet to the test chamber is situated in the bottom part of the back wall. Before entering the test chamber, the air passes through a metallic grid shown in figure 6. This is done to ensure turbulent behavior of the air [2], however it limits the size of the structures in the wind, which will be further analyzed in chapter 3.

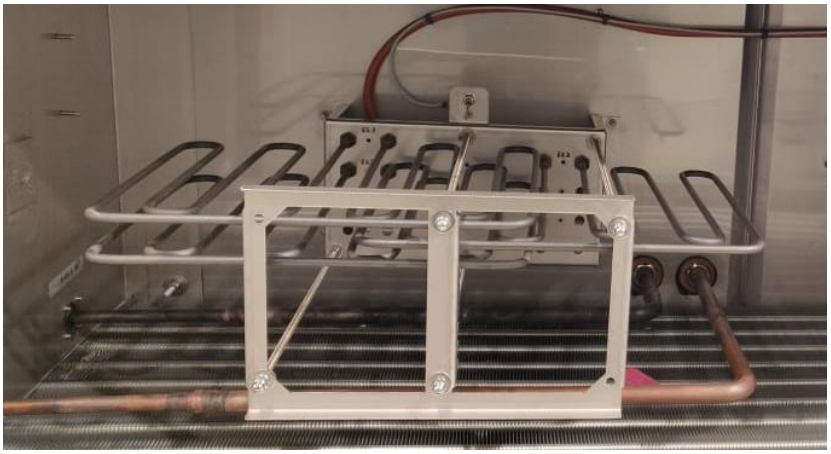

Figure 6. Detail of the metallic grid in the back wall of the test chamber.

2.2 Apparatus

Planning out the experiments requires not only to understand what kind of data is important to collect, but also what resources are needed to conduct said experiments. One of the most important element is the radio mock-up unit acting as heat source, provided by Ericsson AB. The study will try to understand how the airflow is affected around the radio unit as it dissipates heat. The range of wind velocities in the chamber, produced by the fans, are measured with two ultrasonic anemometers. Recording the data and processing it requires many other specialized apparatus that are also described in this section.

2.2.1 Radio mock-up unit

During the tests, the only heat source element inside the chamber is a radio mock-up unit. This section includes a physical and a functional description of said unit. More information on how the radio unit will serve to validate the data output, and how it is a crucial element in the outdoor vs indoor comparison is explained in chapter 3.

Physically, it is composed of an aluminum enclosure in the form of a rectangle, with two larger faces (front and back) and two smaller faces, which make up the sides of the unit. The front side is flat, but the back side is composed of straight vertical aluminum fins that are responsible for almost all the heat dissipation in the unit. Heat is generated inside the unit through two heat mats that are stuck on the flat interior of the aluminum enclosure (marked 1 and 2 in white), and temperature is measured with K type thermocouples (marked 1 to 6 in black). Figure 7 shows the cross section of the unit.

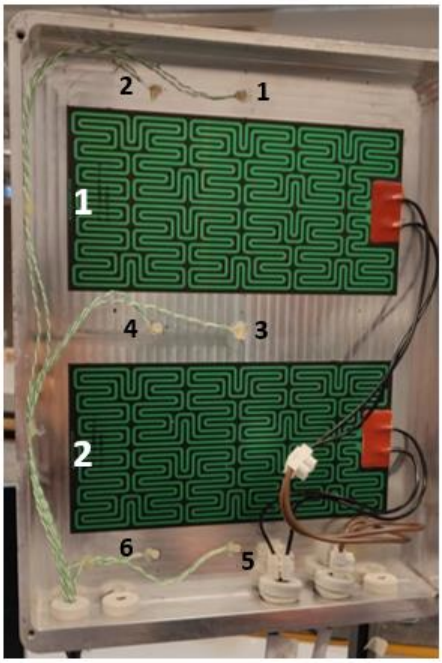

Figure 7. Cross section of the radio mockup unit

Heat mat 1 is powered with 150W, and heat mat 2 with 50W. The power supplied to both of them come out of the unit through the same point, on the bottom left corner, grouped in a larger cable enclosure which keeps them in place. They will then be connected to a data logger.

2.2.2 Ultrasonic Anemometers

The anemometers are developed by 'Gill Instruments' (Lymington, England) and have the catalogue name of WindMaster 3D Ultrasonic Anemometer. From the 'WindMaster Gill user manual', information on the principles of operation, specifications, installation, message formats, inputs and outputs and software configuration can be found. The most basic description of the anemometers is that they are constructed in aluminum and carbon fiber and can perform wind velocity measurements in the three components of the velocity (longitudinal, lateral and vertical) of up to 45m/s.

Figure 8 shows a depiction of a WindMaster 3D ultrasonic anemometer, composed of the measuring devices (transducers) and the shaft that protects them and holds them in place.

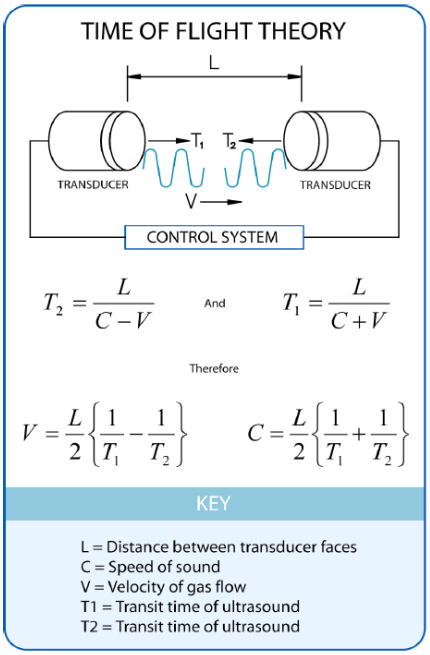

Figure 8. WindMaster 3D ultrasonic anemometer. *Figure 9. Time of flight theory used in ultrasonic anemometers.*

The measurements are taken following the 'time of flight theory', described in figure 9, which measures the time taken for an ultrasonic pulse of sound to travel from an upper transducer to the opposite lower transducer, and compares it with another pulse from the lower transducer to the upper transducer [4].

Another key aspect on how the anemometers function is the axis definition. Figure 10 shows how the axes are physically described on the anemometers;

- U component (longitudinal) is defined towards the direction of the N (north) spar.

- V component (lateral) is defined as 90° anticlockwise from the N reference spar.
- W component (vertical) is defined as vertically up the transducer mounting shaft.

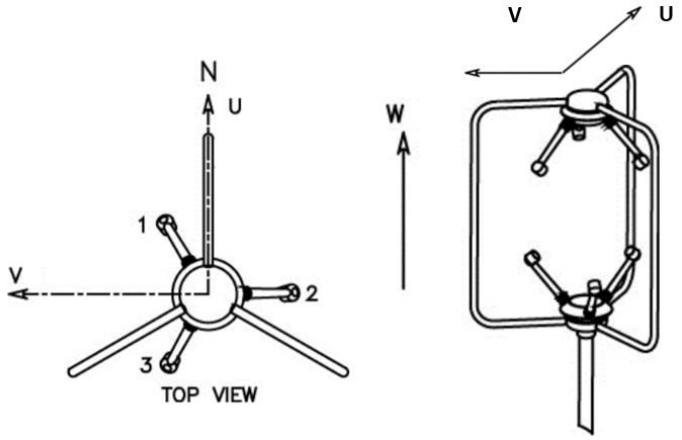

Figure 8. U,V and W axes definition on the ultrasonic anemometers

2.2.3 Other apparatus

More apparatus are needed for the correct collection and processing of measurement data. They are described as follows:

- Converter: Connected to the ultrasonic anemometers and to a computer unit. In charge of converting the ultrasonic readings into formatted wind speed data in the computer. The ADAM 4520 converter model is used, provided by Ericsson AB.
- Datalogger: Connected to the K-type thermocouples and to the same computer unit. In charge of converting thermocouple readings into formatted temperature data in the computer. The Agilent 34972A datalogger model is used, provided by Ericsson AB.
- Power supply unit (PSU): Connected to the power cables in the radio unit. The voltage and the current in the 2 channels is independent and can be tuned manually.
- Computer unit: With the software for both the WindMaster and the Datalogger installed.
- Cabling: Two ethernet cables connect the anemometers and the converters respectively. Two Video Graphics Arrays (VGA) cables connect the converters to a USB drive port, this port is then connected to the computer by two USB cables. Another USB cable connects the datalogger to the laptop.

The location of the elements during the experiments is a key aspect of the design process. Inside the chamber, the goal is to have the minimum amount of apparatus possible, so that they do not interfere with the flow structures created and therefore influence the results. Therefore only the radio mockup unit and the anemometers will be placed inside the chamber. The apparatus described in this section will all be located outside the chamber

and will be connected to the apparatus inside through the grommets in the chamber side wall.

2.3 Experiments

The aim of the experiments is to log airflow data (speed and direction) in the test chamber, for varying power settings of the fans.

The only dependent variable in the tests is airflow. The airflow will depend on fixed variables and independent variables. The fixed variables include; the geometry of the test chamber, the geometry and location of radio mock-up in the test chamber, the temperature of the radio mock-up and the temperature, pressure and humidity ambient indoor values.

The first independent variable is the fan power, which will be tuned manually from the control panel. The 30%, 50% and 100% stepwise increase in fan power is chosen to match previous experiments carried out by the Thermal Design department, and therefore also applied here in order to compare the results. Further explanation on how this is done in chapter 3.

The second independent variable is the orientation of the radio unit around a central pivot point. This is done manually after each test procedure is finished, making sure the central pivot point of the radio and the distance to the anemometers for each test is constant.

2.3.1 Experimental strategy

To characterize the test environment 4 different points are selected in the test chamber, where anemometers are placed. Figure 11 shows the position of the anemometers and the central position of the radio unit, marked with an X.

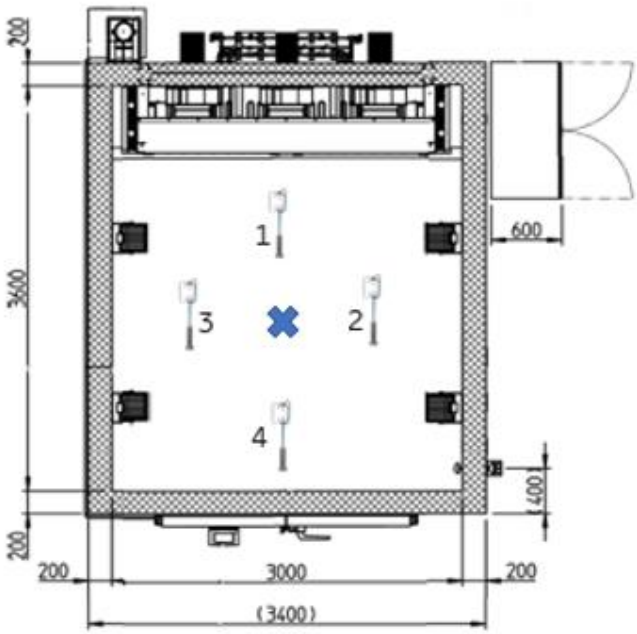

Figure 9. Position of anemometers within the test chamber

The position of the anemometers is selected as such to cover as much of the test space as possible. The anemometers are aligned with the center of the radio in the horizontal plane, at a certain distance from the ground. The radio is placed in the center of the test room so that the measurements are symmetrical. Also it allows to change the orientation of the radio unit, without changing any other parameter.

In theory, the best experimental practice would be to rotate the radio 90° each time, adding to a total of 4 test runs. Because of time and resource limitations, only 3 positions of the radio were tested as described in Figure 12. Changing the orientation of the radio delimits the start of a new test.

Only two anemometers were available to realize the tests, requiring to change their position once to complete a test.

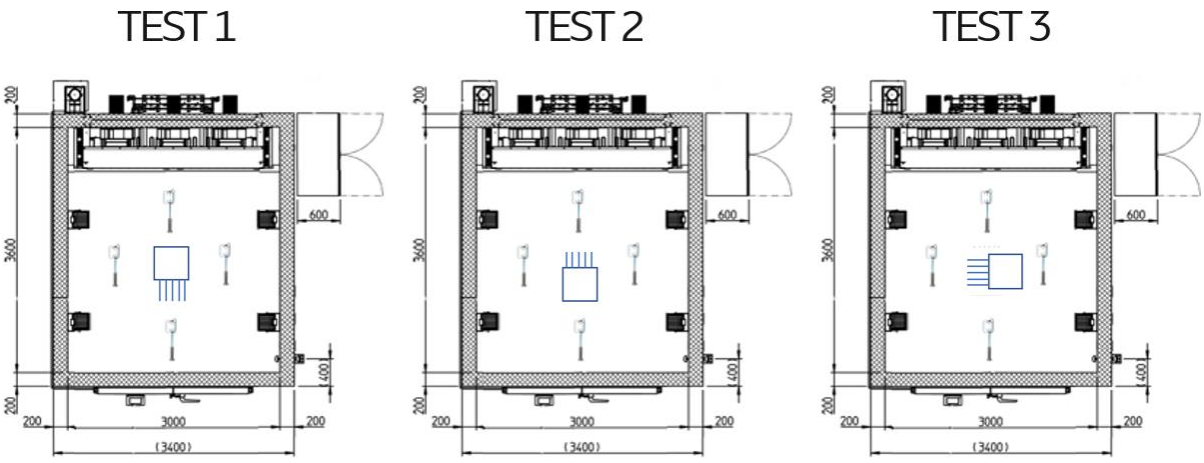

Figure 10. Radio orientations for each test.

2.3.2 Experimental procedure

Figure 13 shows the complete setup for the first experimental run (Test 1), where all the apparatus described in section 2.2. are also shown.

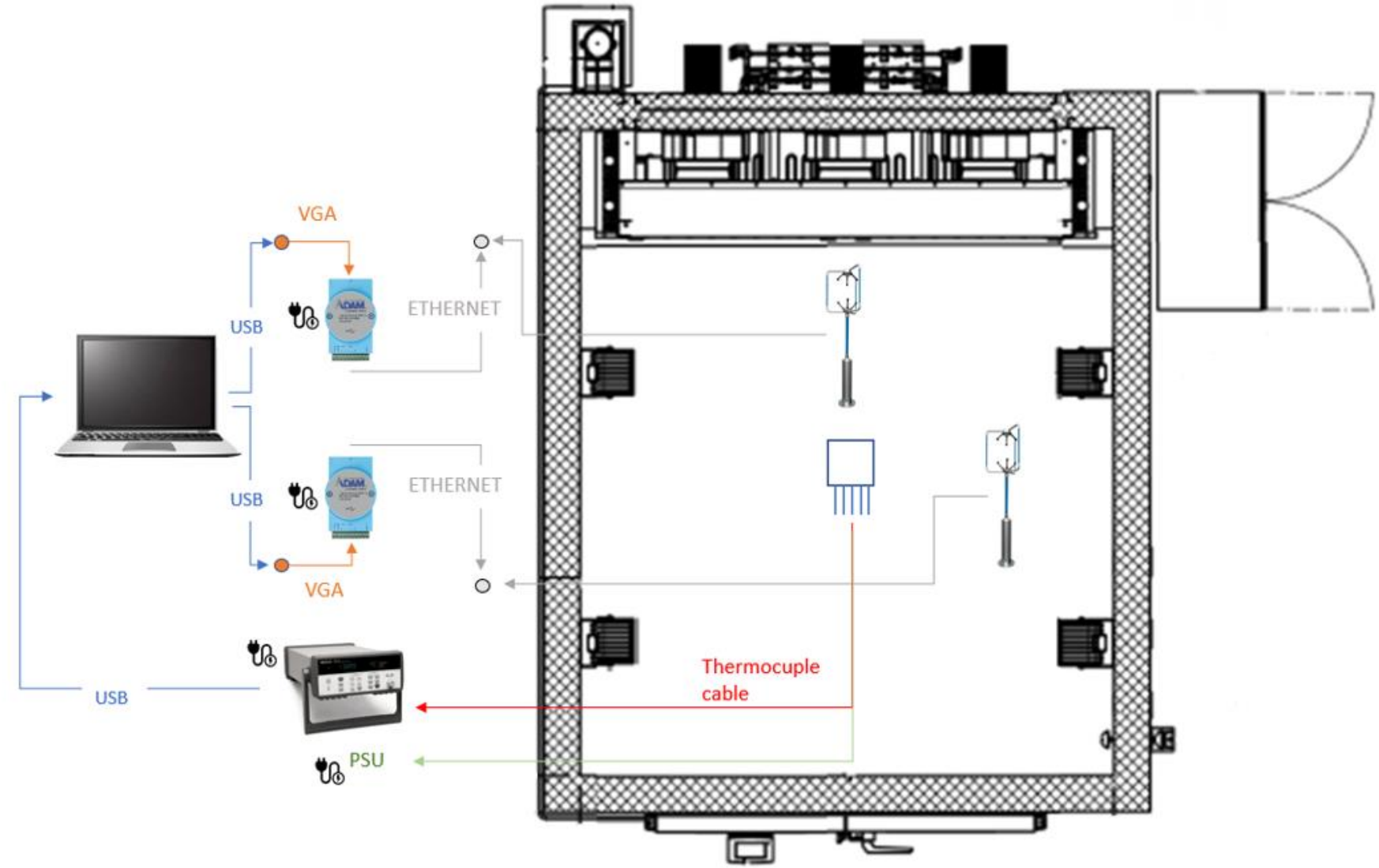

Figure 11. Complete equipment setup for the first run in Test 1.

The experimental procedure is as follows:

1) Set up the equipment as shown in figure 13. Make sure all the outlets in the chamber are fully sealed after putting the apparatus in place.
2) Make sure all software is ready to use and all hardware is fully functioning.
3) Start logging temperature readings (thermocouples should indicate room temperature at this point). Turn on the power supply unit (PSU) for nominal power values, let the temperature in the radio increase until it stabilizes. Around 70°C.
4) Set the parameters of the chamber to 30% fan speed (config.1). Run the program and immediately after start logging for wind speed on both anemometers.
5) Once the thermocouples read a new stabilized temperature for the radio, increase the fan speed to 50% leaving all other parameters constant.
6) Once the thermocouples read a new stabilized temperature for the radio, increase the fan speed to 100% leaving all other parameters constant.
7) Once the thermocouples read a new stabilized temperature for the radio, turn of PSU and let the radio cool down. Keep the fan power to 100%. Keep logging wind speed and temperature.
8) Once the temperature readings are back to ambient temperature, stop the climate chamber (CC) program, stop logging data and save all the files produced.
9) Open the CC and change the position of the anemometers from 1 and 2 to 3 and 4.
10) Repeat steps 3 to 8.
11) Open the CC and change the orientation of the radio 90° clockwise. Fins will now face right wall. Change the position of anemometers back to 1 and 2.
12) Repeat steps 3 to 10.
13) Open the CC and change the orientation of the radio 90° clockwise. Fins will now face front door. Change the position of anemometers back to 1 and 2.
14) Repeat steps 3 to 10.
15) Open the CC and change the orientation of the radio 90° clockwise. Fins will now face left wall. Change the position of anemometers back to 1 and 2.
16) Repeat steps 3 to 10.
17) Test concluded.

2.4 Methods to characterize turbulent flows

In this section, the methods used to characterize the turbulent flow in the climate chamber are explained. First, the relevant theory on turbulent behavior of wind flow is described, where the equations used in the following sections are presented. Then the focus changes to the methods applied to post process the experimental data, in order to derive the parameters that are relevant for the final discussion in chapter 3.

2.4.1 Turbulent flow behavior

For a fluid moving in the turbulent regime of the flow, the velocity vector includes both a mean and a turbulent component. If the flow was laminar, the mean velocity of the flow would correspond to the total velocity, whereas in turbulent flow, turbulent eddies create fluctuations in the velocity vector. The velocity of a turbulent flow can be decomposed into the mean velocity of the flow and the turbulent velocity of the flow, in what is known as Reynolds decomposition [5].

The turbulent eddies in the flow are random, therefore statistical methods are necessary to evaluate said flow. It is important to note that, even though the velocity fluctuations behave as a continuum, the data obtained from measuring said velocity is given as discrete equidistant spaced points, and therefore the following equations can be used to characterize the governing flow:

$$Mean\ velocity: \bar{u} = \frac{1}{N}\sum_{i}^{N} u_i \qquad \textit{Equation 1}$$

$$Turbulent\ fluctuations: u_i' = u_i - \bar{u} \qquad \textit{Equation 2}$$

Where u_i represents each discrete measurement in the velocity measuring series, $\bar{u}$ is the mean component of the velocity, and u_i' is the discrete turbulent component in each velocity measurement.

Calculating the standard deviation of the governing flow can also be done in a discrete way, by applying the statistical tool to the set of velocity fluctuations u_i'. This will give the root-mean-square of the velocity, which indicates the level of turbulence in the flow. The turbulence intensity is a parameter that represents this phenomenon, calculated by dividing the u_{rms} and the $\bar{u}$.

$$u_{rms} = \sqrt{\frac{1}{N}\sum_{i}^{N} (u_i')^2} \qquad \textit{Equation 3}$$

$$Turbulence\ intensity = \frac{u_{rms}}{\bar{u}} \qquad \textit{Equation 4}$$

Boundary layers are solid surfaces in the way of the flow, where the flow behaves in a distinct manner. The definition of boundary layer is known as ‘no slip condition’ where the

velocity of the fluid in the boundary equals 0. The viscosity of the fluid determines the properties of the flow and is responsible for the 'no slip condition', where the fluid stops completely. At a certain distance above the boundary, in the bulk of the fluid, the velocity reaches a constant value (u_∞) [5].

Turbulence is generated by a phenomenon called 'shear', when the free stream of the velocity varies in the vertical coordinate across a surface or boundary. The stronger the shear, the strongest the instability that generates the turbulence. Therefore, the turbulence intensity is higher as the boundary is approached, which means that it is lower in the bulk of the flow [5].

In the climate chamber, the turbulence intensity is the highest at the inlet, as the air is pushed through the metallic grid shown in Figure 6. This will be one of the values calculated in the post processing, which will serve as input for the numerical model.

As the focus of the experiments lies on the bulk of the flow, no further explanation on how the fluid behaves close to a boundary layer will be done. The approach described above is enough for the purpose of the thesis. The post experimental analysis will be based on spectral techniques on the whole array of velocity values.

The most specific characteristic of turbulent flow is that it produces a wide range of turbulent eddies, and therefore a wide range of length scales. Length scales indicate the size of the rotational structures in the flow, they are a key asset in computational analysis as the longest ones serve to delimit the size of the elements in the medium [5]. Focus will be put on finding the values of the longest length scale, known as the Integral Length Scale (ILS) of the flow.

The relative sizes of the length scales indicate the relative energy content of the structures in the flow. The integral length scale is known to represent around 80% of the energy content in the flow. However, turbulent flow always tends to break the longest most energetic length scales into smaller less energetic ones. This means that the amount of longer length scales in the flow is less than that of shorter length scales. The frequency of the integral length scale is the smallest in the flow [6].

As the larger structures break into smaller ones, kinetic energy is handed down in what is known as an energy cascade. A graph of the energy content in the flow vs the frequency of this same structures in the flow is known as Energy Density Spectrum (EDS). A typical EDS for turbulent flow showcases the energy cascade shape, how the larger frequencies correspond to the smaller energy containing structures in the flow [5].

2.4.2 Turbulent wind speeds

The readings from the anemometers correspond to the most important experimental output of the thesis. To find correlations in the wind behavior is what will determine the results of the project. The realization of a numerical model, the comparison with previous indoor experiments in the climate chamber and the comparison with outdoor field data all depend on the correlations found from the turbulent wind readings.

Readings from the anemometers are divided in longitudinal, lateral and vertical wind components (*U,V,W*). The following figure shows an example of the longitudinal values recorded in a complete test routine.

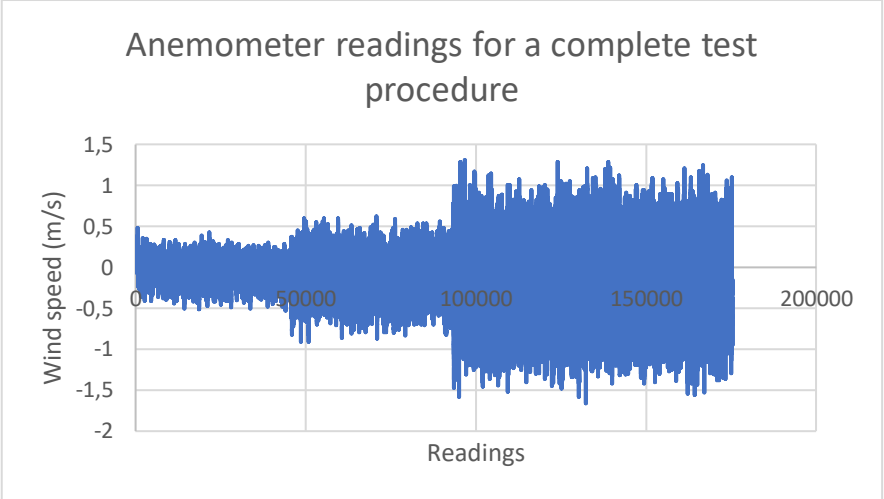

Figure 14 Longitudinal wind speeds for a complete test procedure

Figure 14 shows 3 jumps in wind speed, corresponding to 30%, 50% and 100% fan power respectively. The positive set of wind speed values and the negative set of wind speed values approximately match. By dividing the dataset in 3 subsets, the airflow properties for each fan power can be assessed individually. From this data, three main parameters will be calculated:

- Mean wind speed
- Turbulence intensity
- Integral length scale

2.4.2.1 Mean wind speeds

The first step in the post processing methodology is to calculate the mean wind speed for each fan power, following equation 1. To do this, the set of data is first split in the three fan steps, and then the absolute values for each are found. The last step is to apply the mean formula to each set of data independently.

From the mean wind speed values calculated, a mean characteristic speed for the test chamber can be extracted. This characteristic speed will serve as reference for comparison reasons when looking at turbulence intensities. To calculate it, the front door measurements are taken, corresponding to the highest values measured in the chamber. These results are then averaged and 3 different mean characteristic speeds are found, one for each fan power configuration.

2.4.2.2 Turbulence intensities

As explained in section 2.4.1, turbulence intensities indicate the level of turbulence in the flow. By calculating the values of the turbulence intensities, for every test carried out, a first idea of how the flow develops inside the test chamber can be drafted. This is important as it

will serve to improve the following experimental routines. By knowing how the flow behaves, new positions of the anemometers can be pinpointed to look for new information on the flow and improve the characterization of the test chamber.

Turbulence intensities are also useful when comparing the numerical model and the experimental data. Values for the turbulence intensities from the numerical model can be generated mathematically and be compared with the results found experimentally. This will show how accurate the model is, and how well it describes the environment.

The methodology behind calculating the turbulence intensities is as follows:

- First a Reynolds decomposition of the flow must be done. Following equation 2 the turbulent component of the flow is separated from the mean wind speed values.
- Next is to calculate the root mean squared speed, by taking the absolute values of the turbulent component and using equation 3.
- The final step is to use equation 4 and extract the values for the turbulence intensities, which will differ with the position of the anemometer and with the fan power configuration.

The mean velocity expressed in equation 4 must be the same for all 4 anemometer positions, for each fan power step. This is where the characteristic mean speeds calculated previously come to use, they will serve as common denominator to calculate the turbulence intensities, making sure the comparison is valid.

2.4.2.3 Integral length scale

Pope [6] defined eddies as 'An eddy eludes precise definition but is conceived to be a turbulent motion localized within a region of size *l,* that is at least moderately coherent over this region. The region occupied by a large eddy can also contain smaller eddies'. The size, in terms of length of these structures are referred to as the 'length scales'. Turbulence length scales vary from the size of few millimeters to a few meters in length.

To obtain this parameter it is fundamental to study the Power Spectral Density (PSD) of the data. PSD is a measure of the signal's power content in the frequency domain. It helps ensure that random data can be overlaid and compared independently of the spectral resolution used to measure the data. It is the way to normalize the amplitude of the data by dividing it by the frequency resolution. The frequency resolution is 20Hz for every test in every anemometer.

The first step is to look at the amplitude spectrum of the velocity signal in the frequency domain. To do this, the fast Fourier transform (FFT) is applied on the velocity signal. The Fourier transform gives a mirror image of values in the imaginary domain and the real domain. Focus is done only on real number values [7].

$$Amplitude = abs(fft(U)/L) \qquad \textit{Equation 5}$$

The corresponding frequency domain will be:

$$Freq = Fs/(L * 0{,}5) \qquad \textit{Equation 6}$$

The length of the signal (L) is used to normalize the data, only half the length of the signal is used as frequency domain because half of the results in the Fourier transform where imaginary.

Taking the readings for one of the anemometers in test 1, for 100% fan power, the following amplitude spectrum was obtained;

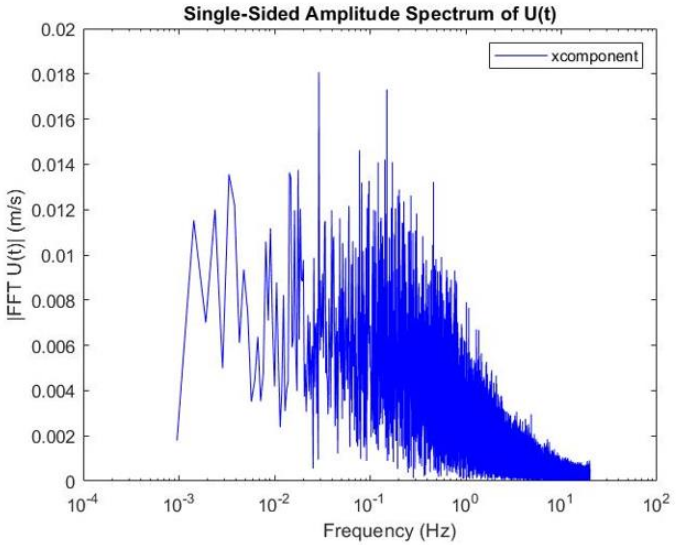

Figure 15. Amplitude spectrum of longitudinal velocity component. 100% fan speed.

In figure 15, the amplitude ranges from 0 to the mean velocity (1m/s), which corresponds to the zero-frequency point. This has been removed from the diagram so that focus can be done on the turbulence energy.

To obtain the power magnitude in the frequency domain, and therefore obtain the PSD; the amplitude spectrum is squared, i.e.:

$$Power = abs(fft(U))^2/L \qquad \textit{Equation 6}$$

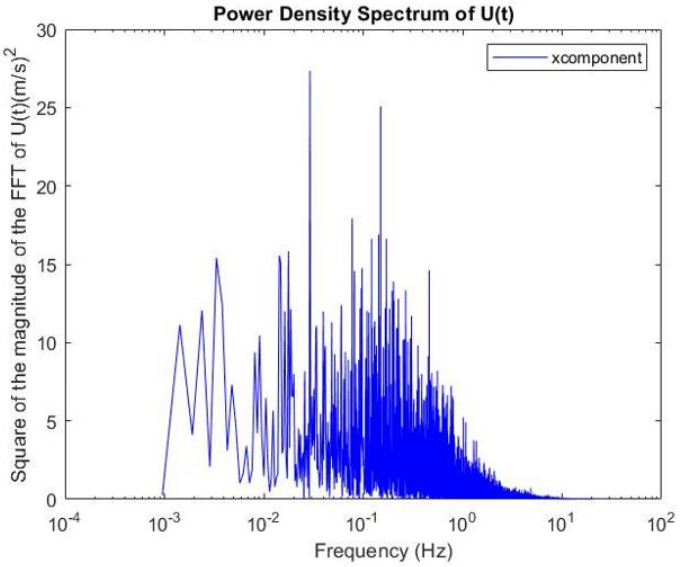

Figure 16 Power Spectral Density of longitudinal velocity component. 100% fan speed.

Figure 16 shows the power spectrum corresponding to the amplitude spectrum in figure 15. It has a similar shape to the amplitude spectrum, because the transformation done only affects the magnitude of the velocity values. By squaring the values, the complete range of power in the spectra is shown, from 0 to around 27 $(m/s)^2$.

From the PSD, the Energy Density Spectrum (EDS) can be obtained. The EDS describes how the energy of a signal is distributed with the frequency. It can be obtained by dividing the power by the frequency of the signal, shown in figure 17.

$$Energy = Power/Frequency \qquad \textit{Equation 7}$$

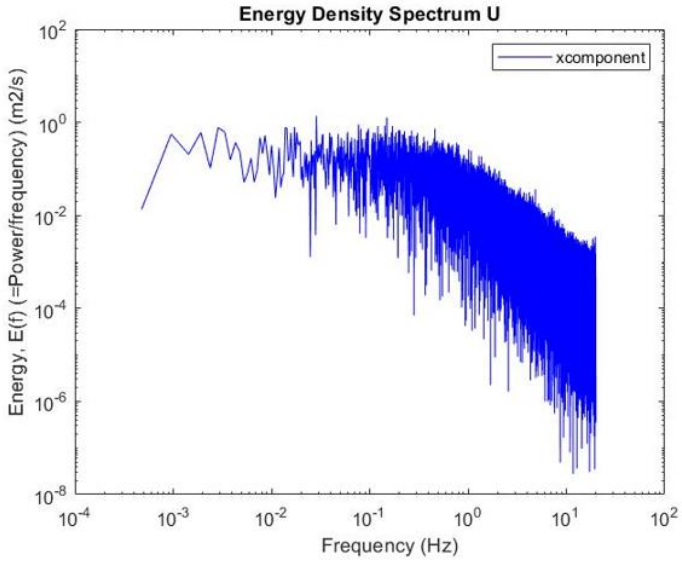

Figure 17. Energy Density Spectrum of longitudinal velocity component. 100% fan speed.

The last step is to filter the EDS so that accurate values of integral length scales can be calculated. To do this, the series of data is split into 20 individual series. For each series, the spectral density is computed in the same way as it has been done for the complete array. The average of the spectral densities is then computed and plotted in the frequency domain.

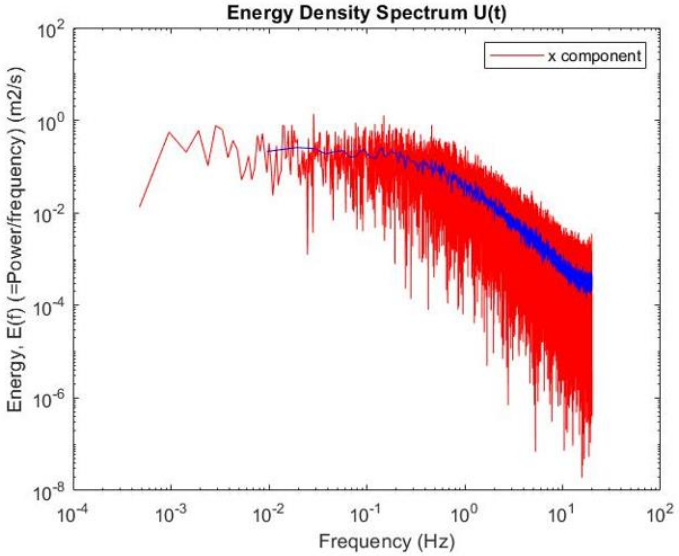

Figure 18. Filtered Energy Density Spectrum (blue) of longitudinal component. 100% fan speed.

Figure 18 shows both the filtered (blue) and original (red) EDS for the same velocity data. It shows how filtering helps to see how the spectra behaves, the horizontal section at the larger energy values is where the integral length scale is calculated from.

To obtain the integral length scale (Λ_x) from this set of data, the following equation is used [8].

$$\Lambda_x = E(f) * abs\left[\frac{U_{mean}}{4 * {\sigma_x}^2}\right] \qquad \textit{Equation 7}$$

- E(f) is obtained by averaging the range of energy values corresponding to when the frequency approaches 0.
- Standard deviation is obtained using the MATLAB function S = std(A), while U_{mean} is obtained from the experimental output data, for the specific position of anemometer used.
- The absolute values of the mean and standard deviation operation are required, because only the magnitude of the integral length scale is relevant, not the direction.
- Using this data processing technique, the integral length scales are obtained for all 4 anemometer positions and fan powers, for the 3 tests conducted.

Chapter 3

Results and discussions

This chapter presents the results and discussions obtained from this thesis project, divided in two parts:

- The first part will cover the results obtained experimentally in the climate chamber.

The results shown here correspond to the experiments described above. These will be referred from now on as indoor experimental results.

- The second part will show a comparison between indoor experimental results and outdoor experimental results. The latter were provided to this project from earlier studies and field trials.

This is done to demonstrate the hypothesis expressed in the goals of the project, which states that the cooling capacity of the wind outdoors is greater than that generated indoors (in the climate chamber).

3.1 Indoor Experimental Results

This section will focus on describing the results obtained from the experimental practices and discussing their relevance in the project. First, the temperature values are described. They are used as reference values within the experimental practices, and to compare between experimental output data and the numerical simulation results.

Then the focus is put on the velocity data obtained, accounting for the 3 fan power configurations (30%, 50% and 100%). The same kind of post processing techniques are applied to all sets of velocity data, towards the goal of obtaining valuable input for the numerical model, and to compare the results obtained from all the experimental runs efficiently. The discussion will be done over the calculated values of mean wind speed, integral length scale and turbulence intensity.

3.1.1 Temperature readings

Temperature readings measured in the radio unit will serve as reference when comparing experimental output data from test to test. A previous set of experiments conducted by

Ericsson AB on the same climate chamber, will serve the purpose of acting as reference, and therefore validate the results obtained experimentally. These set of tests will be referred to from now on as Thermal Design tests. Base case tests and the experimental tests conducted for this work share the following characteristics:

- Radio mock-up unit
- Power input
- Radio position in the CC
- Fan power configuration
- Same thermocouples in same position in radio unit.

The main difference between Thermal Design tests and the tests conducted for this thesis work is that in Thermal Design tests, the stabilization period of the temperature in the radio unit was much longer. These temperature values are esteemed to be more accurate and that is why they serve the purpose of being reference temperature values [9].

These reference values will also be used to validate the numerical simulation results. However it is important to keep in mind that, when comparing experimental values with values generated by the model in the computer, only steady state values can be validated. Steady state refers to state variables that define the behavior of a process and are unchanged with time. In this case, the stable temperature values of the radio unit for each fan power, define the steady state period in the experiments [10].

Steady state values obtained in Thermal Design tests are shown in table 1

	Sensor 1 (°C)	Sensor 2 (°C)	Sensor 3 (°C)	Sensor 4 (°C)	Sensor 5 (°C)	Sensor 6 (°C)
30% fan speed	65,06	64,38	61,09	60,13	52,02	51,80
50% fan speed	60,53	59,69	57,38	56,57	48,75	48,76
100% fan speed	54,58	54,13	52,64	51,70	44,94	44,70

Table 1. Reference values for the steady state temperatures in the radio unit, 30%, 50% and 100% fan power

Table 2 shows the steady state temperature values obtained in the experiments carried out for this thesis project. It is important to mention that, during the test runs, thermocouple number 6 stopped working. This value however can be assumed to be very similar to the readings obtained from sensor 5 (thermocouple 5), as they were redundantly covering the same area in the radio unit

Test 1	Sensor 1 (°C)	Sensor 2 (°C)	Sensor 3 (°C)	Sensor 4 (°C)	Sensor 5 (°C)	Ambient temp (°C)
30% fan speed	66,74	66,18	63,57	62,78	55,11	24,81
50% fan speed	60,85	60,24	58,19	57,39	50,43	24,57
100% fan speed	51,60	51,04	49,75	48,99	43,21	24,56
Test 2	**Sensor 1 (°C)**	**Sensor 2 (°C)**	**Sensor 3 (°C)**	**Sensor 4 (°C)**	**Sensor 5 (°C)**	**Ambient temp (°C)**
30% fan speed	65,26	64,74	62,10	61,34	53,92	24,83
50% fan speed	59,91	59,28	57,07	56,38	49,32	24,53
100% fan speed	51,64	50,96	49,44	48,72	42,44	24,45
Test 3	**Sensor 1 (°C)**	**Sensor 2 (°C)**	**Sensor 3 (°C)**	**Sensor 4 (°C)**	**Sensor 5 (°C)**	**Ambient temp (°C)**
30% fan speed	66,79	66,20	63,50	62,65	54,78	24,80
50% fan speed	61,84	61,25	59,04	58,23	50,86	24,50
100% fan speed	53,23	52,79	51,46	50,70	44,36	24,42

Table 2. Steady state temperatures in the radio unit for the thesis project, 30%, 50% and 100% fan power.

Table 3 shows the difference in temperature readings between both experimental procedures. The values where calculated by subtracting the averaged stable temperature values in table 2 from the stable temperature readings shown in table 1.

	Test 1 °C	Test 2 °C	Test 3 °C
30% fan speed	+2,34	+0,95	+2,25
50% fan speed	+0,85	+0,42	+1,65
100% fan speed	+2,66	+2,96	+1,10

Table 3. Stable temperature difference.

All of the values are positive, which indicates that the temperatures during the thesis experiments still needed of some more time to stabilize fully, but where all moving towards the reference temperatures. Table 3.3 also shows how all experiments conducted follow the same trend for the different fan powers. The results obtained by comparing the change in temperature to an accurate reference, indicates that the experiments have high internal validity and that control was established successfully in all tests. The difference between the measurements can be associated to the accuracy of the thermocouples (+/-1°C).

3.1.2 Airflow

This section presents the experimental characterization of the airflow in the climate chamber, through values of mean wind speed, turbulence intensities and integral length scales. Figure 14 shows a 3D image of the test chamber, how the air enters and leaves the test space. This will help explain the results obtained in this section.

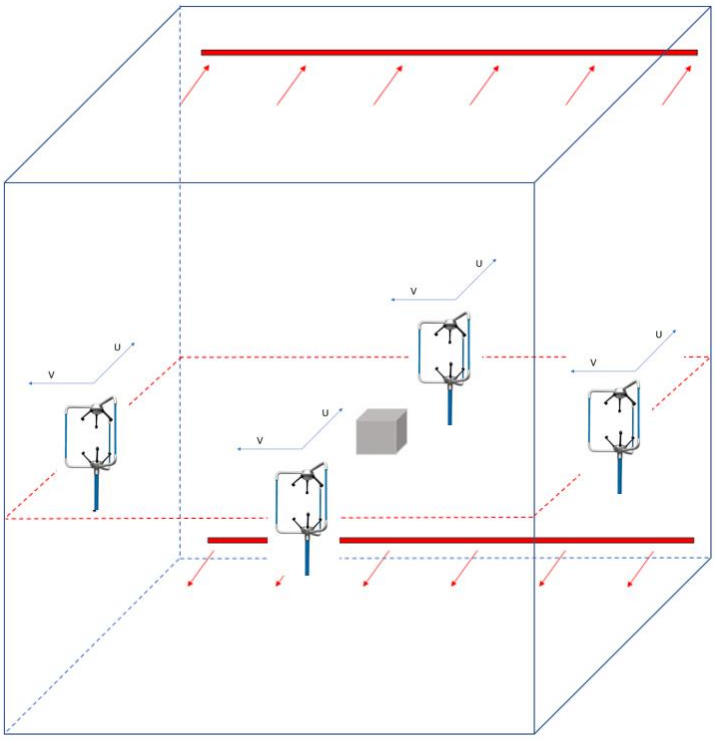

Figure 12. 3D image of the test chamber during a test.

3.1.2.1 Mean wind speed indoors

A total of 12 graphs compose the complete information on the values of the wind speed for the longitudinal axis of the anemometer.

Table 4 shows all mean wind speed values (in m/s) for every test configuration and position in a summarized manner.

Test 1	30% fan power	50% fan power	100% fan power
Back wall	0,13	0,25	0,40
Left wall	0,15	0,26	0,47
Right wall	0,11	0,19	0,34
Front door	0,35	0,58	1,06
Test 2	**30% fan power**	**50% fan power**	**100% fan power**
Back wall	0,11	0,18	0,31
Left wall	0,14	0,23	0,49
Right wall	0,09	0,18	0,32
Front door	0,34	0,59	1,03
Test 3	**30% fan power**	**50% fan power**	**100% fan power**
Back wall	0,12	0,17	0,30
Left wall	0,13	0,22	0,44
Right wall	0,08	0,14	0,24
Front door	0,32	0,62	0,99

Table 4. Summarized mean wind speed values (m/s) for every fan configuration and position tested.

For all the tests conducted, the values of the wind speed in the front door were larger than for the rest of the room. This can be explained because the air inlet to the test chamber is situated close to ground level in the back wall of the chamber. The air will first travel along the ground floor until it bumps into the front wall, it will then ascend vertically, creating vortices into the rest of the chamber. The wind speed values captured by the front anemometer are the closest measured values to the inlet, where the air is the fastest.

It is interesting to see how the values for the left wall are consistently higher than the values for the right wall, which may indicate that air flow is not symmetric, even though the flow domain is. This can be due to small differences in fan performance.

From table 4 it can also be seen that as the fan power increases, the variability in readings increases. This can be attributed to the apparatus, as the precision of the anemometer lowers for higher wind speed values [4].

Other factors inside the chamber also affect these readings; including the distance at which the anemometers are from the radio (1 meter), and the mounting apparatus used to hold the equipment in place, which affects the structure of the flow. It is difficult to pinpoint how the radio affects the wind speed readings from these tests, there is almost no relationship that can be extracted from the differences in the orientation of the radio.

To obtain the characteristic speed in the chamber, the wind speed values in the front door position are selected. These are the highest speed values in all tests, as the air coming out of the inlet reaches the front door position first in the flow cycle. It is not until the air bounces against the chamber front wall, that it reaches the other 3 positions, losing energy on its way. Values calculated for the characteristic mean wind speed are shown in table 5.

	Characteristic speed in test chamber
30% fan power	0,34
50% fan power	0,60
100% fan power	1,03

Table 5. Characteristic speed (m/s) in the test chamber for the 3 fan power configurations.

3.1.2.2 Turbulence intensities indoors

For every test, 12 values for the root mean squared speed are calculated. This correspond to the 4 different anemometer positions for the 3 fan power configurations. The values calculated are shown in table 6 (in m/s).

Test 1	30% fan power	50% fan power	100% fan power
Back wall	0,07	0,11	0,18
Left wall	0,07	0,12	0,234
Right wall	0,06	0,10	0,178
Front door	0,07	0,11	0,197
Test 2	**30% fan power**	**50% fan power**	**100% fan power**
Back wall	0,05	0,08	0,15
Left wall	0,05	0,08	0,16
Right wall	0,05	0,08	0,17
Front door	0,07	0,12	0,23
Test 3	**30% fan power**	**50% fan power**	**100% fan power**
Back wall	0,05	0,08	0,14
Left wall	0,05	0,10	0,17
Right wall	0,04	0,08	0,13
Front door	0,08	0,12	0,25

Table 6. Root mean squared speeds (m/s) for every test conducted indoors.

As the fan power increases, the root mean squared speeds increase. In test 2 and 3, a similar pattern to the values obtained in table 5 is observed. This is an expected result, as the fluctuations due to the turbulence in the flow are carried in the wind structures, and therefore follow the same pattern as the mean wind speed does.

Test 1 however accounts for a slightly different distribution, where the values in the back wall and in the front wall are closer. This could be due to the orientation of the anemometers, a small change in orientation can capture a small difference in wind structures.

Test 1	30% fan power	50% fan power	100% fan power
Back wall	19,1	18,3	17,9
Left wall	20,0	20,5	22,7
Right wall	17,4	16,2	17,3
Front door	19,7	17,8	19,1
Test 2	**30% fan power**	**50% fan power**	**100% fan power**
Back wall	13,8	13,2	14,3
Left wall	13,8	13,3	15,5
Right wall	13,5	14,0	16,6
Front door	21,5	20,2	21,9
Test 3	**30% fan power**	**50% fan power**	**100% fan power**
Back wall	13,8	12,8	13,7
Left wall	15,6	16,0	16,3
Right wall	12,6	12,5	12,8
Front door	22,4	20,2	23,9

Table 7. Turbulence intensities (%) for every test conducted indoors.

Using equation 4, the values obtained in table 5 and the ones obtained in table 6, the turbulence intensities are calculated. Table 7 presents the values of the turbulence intensities for every experimental practice conducted indoors.

As table 6 suggests, the values of the turbulence intensities present in table 7 are very different for test 1 than what they are for test 2 and test 3. The hypothesis behind these results is that the orientation of the anemometers was slightly different for test 1. Turbulence intensity values are greatly influenced by the turbulent component of the wind, which is unpredictable, while the frequency of measurements is high and the wind speed values measured are small.

Even though the values for turbulence intensity do not seem to change as the fan power is increased, the flow is becoming more turbulent in the test chamber. These values do not change because the mean velocity is also increasing, but the root mean squared speed does increase with fan power.

3.1.2.3 Integral length scales indoors

The values of the integral length scales for every test, anemometer position and fan speed are presented in table 8.

Test 1	30% Fan Speed	50% Fan Speed	100% Fan Speed
Back wall (m)	0,03	0,03	0,02
Left wall (m)	0,03	0,05	0,05
Right wall (m)	0,01	0,03	0,04
Front door (m)	0,04	0,05	0,06
Test 2	**30% Fan Speed**	**50% Fan Speed**	**100% Fan Speed**
Back wall (m)	0,03	0,02	0,02
Left wall (m)	0,04	0,04	0,06
Right wall (m)	0,01	0,02	0,02
Front door (m)	0,06	0,08	0,09
Test 3	**30% Fan Speed**	**50% Fan speed**	**100% Fan Speed**
Back wall (m)	0,03	0,02	0,02
Left wall (m)	0,03	0,03	0,04
Right wall (m)	0	0,01	0,01
Front door (m)	0,07	0,07	0,09

Table 8. Integral length scales (m) for every test conducted indoors.

As mentioned previously, the integral length scales represent 80% of the energy in the airflow. These structures are only found in the lowest frequencies, as they quickly break down into smaller and smaller less energetic structures [6]. It is a good point of comparison as it showcases a fixed phenomenon in the randomness of the turbulent behavior in the flow.

From the data obtained, the clearest trend that can be seen is that the values in the front door correspond to the longest length scales. This is expected, as the anemometers in the front door position are exposed to the most energetic wind structures, as shown from the results obtained throughout the analysis. After the wind flows back towards the back wall and past the other anemometer positions, the structures have broken down into smaller ones.

It is interesting to see that, even though the test chamber is physically symmetrical, and the position of the radio is exactly in the center of the test space, the left wall has higher values of integral length scales than the right wall. This can be due to several reasons, the first being that the performance of the fans to the right and to the left may be slightly different. This cannot be confirmed as the calibration of the chamber only focused on temperature and humidity values, the fans performance was never checked. It could also mean that there was a physical element in the right wall which was not present in the left wall during the tests. Possibly the cables that came out of the anemometers and through the grommets of the chamber had an effect on breaking the wind structures even further.

3.1.3 Experimental improvements

The experiments described on this report only constitute the first series of tests that were originally planned to be conducted on the climate chamber. Unfortunately, no more tests could be conducted in the whole span of the thesis, and therefore improvements can only be speculated upon. Nonetheless there are some clear points to improve on, based on the post processing of the data, that can produce better experimental output results and therefore procure a better characterization of the climate chamber:

- The temperature on the radio unit should have been left to stabilize for a longer period of time.

The numerical model does not account for transient airflow behavior, and therefore the comparison between experimental and numerical will be more precise if the temperatures on the radio properly stabilize.

- Fix thermocouple number 6.

It stopped working throughout the tests, but this does not discredit the data collected as thermocouple number 5 reads values that are redundant for both. The comparison of the temperature values is done in pairs, thermocouples 1 and 2 read a different temperature range than thermocouples 3 and 4 and thermocouples 5 and 6.

Improvements on the experimental setup

- Make sure that test number 4 is carried out, the information for when the radio unit faces the left wall must be collected.
- Smaller mounting equipment must be used inside the climate chamber, they have to still maintain the weight of the apparatus, while affecting the airflow as least as possible.
- Shorten the distance of the anemometers to the radio unit, trying to see in more detail how the airflow around the radio unit is affected by dissipation of heat.
- Change the orientation of the anemometers. After understanding how the airflow behaves inside the chamber, the anemometers can be positioned so that the longitudinal axis follows the direction of the flow.

This is the biggest improvement to the tests, because the experiments described above do not consider the direction towards which the anemometers are facing. In fact, this is the biggest difference between test 1, test 2 and test 3; the velocity spectra obtained for each test does not exactly match, because the anemometers where not facing towards the same direction.

3.2 Outdoor experimental results

Wind velocity data obtained over 10 days from a similar experimental practice carried out by Ericsson AB outdoors, is analyzed and compared to the velocity data obtained indoors (in the climate chamber). The main reason behind doing this analysis is to prove the hypothesis stating that the cooling capacity of the wind outdoors is greater than that obtained from the airflow in the climate chamber, for the same conditions. This analysis will serve to understand how differently the energy content of the wind is and how this difference is quantified.

3.2.1 10 days comparison

Experimental outdoor tests conducted by Ericsson and the ones conducted for this thesis work share the following characteristics:

- Radio mock-up unit
- Power input
- Same anemometers
- Same distance of anemometer and radio unit

Comparing indoor and outdoor data is a way of learning how differently the environment influences the airflow. However, outdoor values cannot serve as reference for indoor data because of a large number of factors that are present outdoors that are not present indoors. The comparison will be done focusing on the length scales and the energy content of the wind structures.

To calculate the integral length scales, the same approach as with the indoor data is used. To fully understand how the energy content in the wind changes per day, all of the variables present in the Roach equation 7 [8] will be presented per day. Even though the positions of the radio and the anemometers are unchanged during the 10 days, every day represents a different set of data, every day is different. It has no physical meaning to average the values from day to day.

	Day 1	Day 2	Day 3	Day 4	Day 5	Day 6	Day 7	Day 8	Day 9	Day 10
$E(f)$ **(m/s²)**	5,13	4,87	3,15	3,05	4,75	3,51	3,48	4,43	3,96	5,02
U_{mean} **(m/s)**	1,61	1,40	1,17	0,78	0,56	1,09	0,52	0,66	1,02	2,01
${\sigma_x}^2$ **(m/s)**	2,21	1,61	0,99	0,82	1,16	1,11	0,78	0,96	1,08	1,87
Λ_x (m)	**0,93**	**1,06**	**0,93**	**0,72**	**0,57**	**0,86**	**0,58**	**0,76**	**0,93**	**1.35**

Table 9. Integral length scales and variables in the Roach equation for every day outdoors

Table 9 shows how all variables are different for different days, showing that every day must be treated as a different set of values. Even though the mean wind speed and standard deviation are different for every day, the range is smaller than that obtained for

the energy values. The biggest change in integral length scale corresponds to the energy content in the structures of these scales.

The frequency range for which the energy values are calculated corresponds to the horizontal section of the spectra in each EDS. This frequency range is small, but it corresponds to the wind structures that contain 80% of the energy on the flow. The EDS plot below shows the filtered EDS for each day plotted together. The behavior of the flow is better explained when looking at this graph.

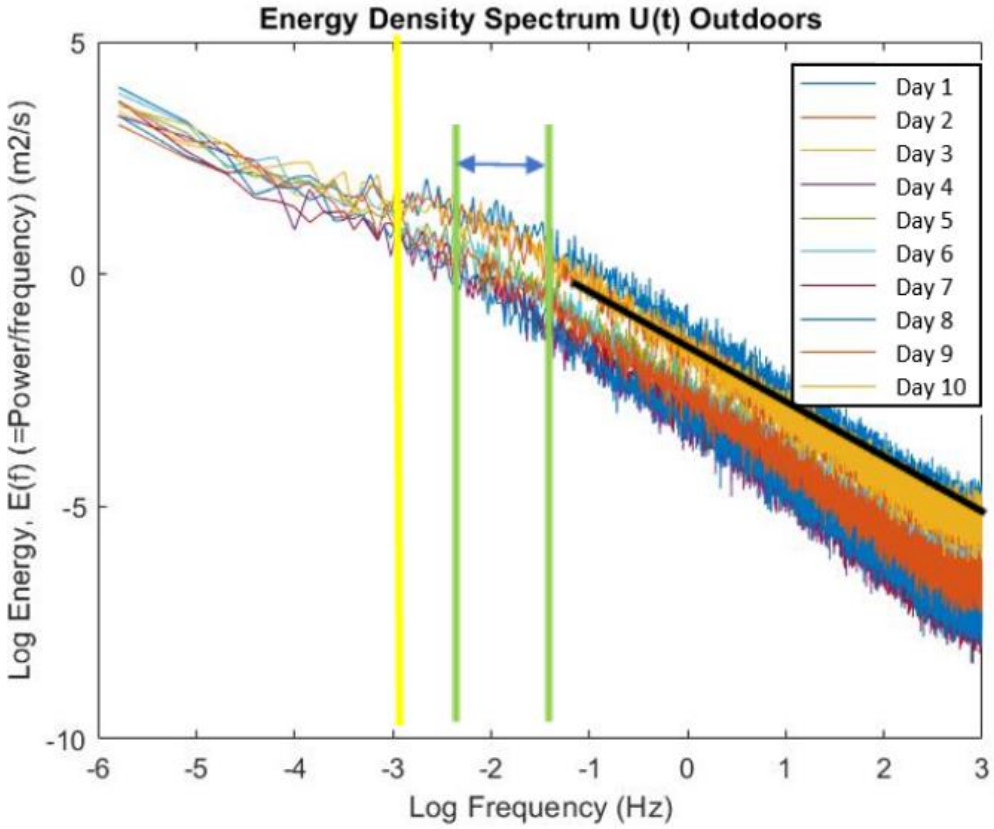

Figure 13. Energy Density Spectra of the 10 filtered outdoor days.

First of all, the black straight line represents the Kolmogorov gradient, slope of -5/3. The Kolmogorov law states that 'energy is transferred in scale by nonlinear process, as a spectral cascade, until it dissipates by viscosity'. This means that the energy transfer is dependent on the viscosity of the flow, and that it will follow the shape described by Kolmogorov if the flow is assumed to be homogenous and isotropic [11].

The yellow vertical line corresponds to the smallest frequency captured in the EDS, 10^{-3} Hz or 0,001Hz. This is the first frequency point for which an energy value is obtained. The values for the frequency range in which the integral length scales are captured are shown in green, from $10^{-2,5}$ Hz to $10^{-1,5}$ Hz or from 0,0032Hz to 0,032Hz. This range of values is selected as it corresponds to the horizontal section in the spectra, where structures capture up to 80% of the energy. It corresponds to the same range of values calculated for the integral length scales indoor, and therefore makes the comparison valid.

3.2.2 Indoor vs outdoor comparison

It is already stated that both experiments are similar in terms of procedure and methodology, therefore the only variable which must differ should be the one that we are interested in analyzing. To do this, the comparison must be done between scenarios with the same wind speed indoors and outdoors. Table 10 shows the closest values obtained indoors to what the wind speed is like outdoors, corresponding to those measured in the front door at 100% fan power.

However there are 3 more days outdoors, where the mean wind speeds also match the indoor measured ones. Days 5, 7 and 8 correspond to a similar wind speed than that measured for 50% fan speed in the front door of the chamber. This is represented in table 11.

	Mean wind speed [m/s]	Integral Length Scale [m]
Test 1 – Front door – 100%	1,06	0,06
Test 2 – Front door – 100%	1,03	0,09
Test 3 – Front door – 100%	0,99	0,09
Day 6	1,09	0,86
Day 9	1,02	0,93

Table 10. Mean windspeed values and integral length scales for 100% values, day 6 and day 9.

	Mean wind speed (m/s)	Integral Length Scale (m)
Test 1 – Front door – 50%	0,58	0,05
Test 2 – Front door – 50%	0,59	0,08
Test 3 – Front door – 50%	0,62	0,07
Day 5	0,56	0,86
Day 7	0,52	0,93
Day 8	0,66	0,76

*Table 11. M*ean windspeed values and integral length scales for 50% values, day 5, day 7 and day 8.

For the same mean wind speed, the integral length scale values in the climate chamber are around 10 times less than those obtained in the outdoors. This means that the energy content in the structures outdoors is higher than those generated indoors. This serves to demonstrate the hypothesis mentioned throughout the report, confirming that the cooling capacity of the wind outdoors is greater than that generated indoors. To find out a specific number that relates both scenarios require of a much more detailed analysis on every factor influencing the wind outdoors and indoors, and therefore they will not be qualitatively compared any further in this project.

The reason behind this result could be explained by looking at the source of the wind in both scenarios. In the climate chamber, the longest length scales are delimited first by the diameter of the fans, and secondly by the size of the aluminium grid which is placed right before the inlet. Both components break the wind structures before it even enters the test chamber. In the outdoors, the wind is generated by the changes of pressure in the atmosphere, which does not limit the size of the structures. This means that the outdoor wind is composed of larger structures with more energy, and therefore can provide a greater cooling capacity than the indoor air can.

Chapter 4

Conclusions and recommendations

This thesis report has focused on the experimental characterization of wind generated in a climatic chamber, on post processing the data obtained and comparing this data to outdoor wind conditions. As explained in the first chapter, all of this work is only half of the total work developed for the project 'Towards a Virtual Climate Chamber', the second half regards the numerical model developed and the results obtained from it.

The conclusions will include both the ones obtained from this project, and the ones obtained from comparing numerical and experimental results, to give a broader image of how the whole enterprise has been developed. The recommendations will be based on improving the experimental procedure conducted and the following steps 'Towards a Virtual Climate Chamber'.

4.1 Conclusions

The original hypothesis has been demonstrated with the results of the comparison in section 3.2.2. For the same mean wind speeds, the wind outdoors has a greater cooling capacity than that of the wind structures produced in the climate chamber. The energy content in the integral length scale, is of about one order of magnitude greater outdoors than it is indoors.

Many other parameters affect the wind outdoors, and therefore no clear constant comparing both scenarios can be obtained yet. Effects of heat dissipation by radiation must be compared with the effect of the integral length scales, to try to better understand the cooling capacities of the wind outdoors.

Inside the climate chamber, the integral length scales obtained did not vary much with radio orientation, it was not possible to see how heat dissipation from the unit affected the flow based on this parameter.

Regarding the numerical model;

- The temperature readings match the ones obtained in the climate chamber for the 50% fan power configuration.

- The mean speed obtained for 50% fan power is 0,6m/s, same as the characteristic speed found experimentally for 50% fan power.
- By focusing on the volume of interest around the radio, the energy density spectra calculated shows a similar distribution to the one found experimentally. The distribution in energy content in the wind structures also behaves as stated by Kolmogorov, an isotropic turbulent energy cascade with a -5/3 slope.
- Values for the turbulence intensities calculated by the model for the 50% fan power scenario, vary with a 5% difference when compared to the experimental ones. This is the biggest difference between both, but it is expectable as the turbulence intensity is greatly affected by the randomness of the turbulent flow, parameter which is not possible to model.
- Values for the integral length scales calculated by the model for the 50% fan power scenario, are found to be in the same order of magnitude as the ones obtained experimentally, to 2 decimal places.

In conclusion, and when comparing the 50% fan power configuration, the values obtained for the experimental and numerical experiences are relatively similar. This means that the numerical model is able to predict wind behavior inside the climate chamber quite robustly for this specific configuration.

However, there are still many improvements to make in the model, the most important one associated to how the thermal dissipation from the radio unit affects the wind flow, for every orientation of the unit.

4.2 Recommendations

Repeat the experiments so that:

- The anemometers are closer to the radio unit.

Meaning that the effect of how the heat transfer affects the wind flow is better studied. To look at different spectral parameters is also recommendable.

- The velocity distribution of the air flow at the inlet is quantified.

The values of the wind velocity at the inlet of the test chamber where never measured, by doing so, better boundary conditions can be specified in the numerical model.

- Minimize the effect of apparatus on the airflow.

The results of the experiments were influenced by the anemometer stands and radio stand. The equipment holding everything in place should be as slim as possible, as it greatly disturbs the wind flow.

In conclusion, the first step ‘Towards a Virtual Climate Chamber’ has been taken, it will depend on future work to successfully complete and test the model.

References

[1] Encyclopedia Britanica. *Sociology, social change*. URL: https://www.britannica.com/topic/social-change. 1998. (Visited on 9/06/2020).

[2] Vötsch Industrieteknik. *Operating manual – Temperature and climate test chamber VCZ 50040 – S.* 2015.

[3] LaboTest. *Kalibrering av temperature och fuktsystem*. 2020

[4] Gill Instruments Limited, WindMaster 3D Ultrasonic Anemometer manual, Hampshire, 2010.

[5] Massachusetts Institute of Technology (MIT). ”*Velocity profiles and turbulence theory*”. URL: http://www.mit.edu/course/1/1.061/www/dream/SEVEN/SEVENTHEORY.PDF (visited on 25/01/2020).

[6] Stephen B. Pope. ”Turbulent flows”. In: *Cambridge University Press*. 2005, Page 183.

[7] Lamyaa A. El-Gabry, Douglas R. Thurman and Phillip E. Poinsatte. ”Procedure for determining turbulence length scales using hot wire anemometry”. In: *Nasa Technical Report Server.* 2014.

[8] P.E. Roach. ”The generation of nearly isotropic turbulence by means of grids”. In: *International Journal of Heat and Fluid Flow.* 1987

[9] Thermal Design Department at Ericsson AB, Kista. Outdoor experiments on mock-up radio unit. 2007.

[10] Y.Y. Liang, J.C. Hu, J.P. Chen Y.G. Shen and J.Du. ”A transient thermal model for full sized vehicles climate chamber”. In: *Energy and Buildings.* 2014.

[11] Department of Mathematical Sciences, Loughborough University, UK. ”*Kolmogorov’s 5/3 law*”. URL: http://www.navier-stokes-equations.com/space-scale-turbulence;focus=CMTOI_de_dtag_hosting_hpcreator_widget_Download_14855856&path=download.action&frame=CMTOI_de_dtag_hosting_hpcreator_widget_Download_14855856?id=184137. (visited on 15/03/2020).

[12] Yuvarajendra Anya Reddy. ”Towards a Virtual Climate Chamber – Numerical study and model’’. Linköping university, in Ericsson AB.